



HAL
open science

Unraveling the ubiquitome of the human malaria parasite

Nadia Ponts, Anita Saraf, Duk-Won D. Chung, Alona Harris, Jacques Prudhomme, Michael P. Washburn, Laurence Florens, Karine G. Le Roch

► **To cite this version:**

Nadia Ponts, Anita Saraf, Duk-Won D. Chung, Alona Harris, Jacques Prudhomme, et al.. Unraveling the ubiquitome of the human malaria parasite. *Journal of Biological Chemistry*, 2011, 286 (46), pp.40320-40330. 10.1074/jbc.M111.238790 . hal-02647761

HAL Id: hal-02647761

<https://hal.inrae.fr/hal-02647761>

Submitted on 29 May 2020

HAL is a multi-disciplinary open access archive for the deposit and dissemination of scientific research documents, whether they are published or not. The documents may come from teaching and research institutions in France or abroad, or from public or private research centers.

L'archive ouverte pluridisciplinaire **HAL**, est destinée au dépôt et à la diffusion de documents scientifiques de niveau recherche, publiés ou non, émanant des établissements d'enseignement et de recherche français ou étrangers, des laboratoires publics ou privés.

Unraveling the Ubiquitome of the Human Malaria Parasite^{*[S]}

Received for publication, March 9, 2011, and in revised form, September 13, 2011. Published, JBC Papers in Press, September 19, 2011, DOI 10.1074/jbc.M111.238790

Nadia Ponts⁺¹, Anita Saraf^{S1}, Duk-Won D. Chung[‡], Alona Harris[‡], Jacques Prudhomme[‡], Michael P. Washburn^S, Laurence Florens^S, and Karine G. Le Roch⁺²

From the [‡]Department of Cell Biology and Neuroscience, University of California, Riverside, California 92521 and the ^SStowers Institute for Medical Research, Kansas City, Missouri 64110

Malaria is one of the deadliest infectious diseases worldwide. The most severe form is caused by the eukaryotic protozoan parasite *Plasmodium falciparum*. Recent studies have highlighted the importance of post-translational regulations for the parasite's progression throughout its life cycle, protein ubiquitylation being certainly one of the most abundant. The specificity of its components and the wide range of biological processes in which it is involved make the ubiquitylation pathway a promising source of suitable targets for anti-malarial drug development. Here, we combined immunofluorescent microscopy, biochemical assays, *in silico* prediction, and mass spectrometry analysis using the multidimensional protein identification technology, or MudPIT, to describe the *P. falciparum* ubiquitome. We found that ubiquitin conjugates are detected at every morphological stage of the parasite erythrocytic cycle. Furthermore, we detected that more than half of the parasite's proteome represents possible targets for ubiquitylation, especially proteins found to be present at the most replicative stage of the asexual cycle, the trophozoite stage. A large proportion of ubiquitin conjugates were also detected at the schizont stage, consistent with a cell activity slowdown to prepare for merozoite differentiation and invasion. Finally, for the first time in the human malaria parasite, our results strongly indicate the presence of heterologous mixed conjugations, SUMO/UB. This discovery suggests that sumoylated proteins may be regulated by ubiquitylation in *P. falciparum*. Altogether, our results present the first stepping stone toward a better understanding of ubiquitylation and its role(s) in the biology of the human malaria parasite.

Malaria is one of the most lethal infectious diseases. Half of the world's population is at risk, leading to about 250 million malaria cases and one million deaths every year (see the World Health Organization Web site). The most severe forms of malaria, leading to death, are caused by the protozoan parasite *Plasmodium falciparum*. Despite significant advances in the research against malaria, many aspects of the parasite's biology remain obscure. Recent studies have highlighted the impor-

tance of post-translational regulations for the parasite's progression throughout its life cycle (reviewed in Ref. 1). Among those, protein ubiquitylation is certainly one of the most abundant post-translational modifications of proteins. Ubiquitylation is classically involved in numerous crucial biological processes in eukaryotic cells in a proteasome-dependent or -independent manner. The specificity of its components and the wide range of biological processes in which it is involved make the ubiquitylation pathway an important source of suitable targets for drug treatments (see Ref. 2 for a review). Proteasome inhibitors are indeed promising drugs to treat cancer and both autoimmune and infectious diseases (see Ref. 3 for a review). In the particular case of *Plasmodium*, the proteasome inhibitors salinosporamide-A (4), bortezomib (5), and MLN-273 (6) have been shown to be efficient antimalarials. In addition to their cellular roles, the components of the ubiquitin system are involved in many host-pathogen interactions. Pathogens often utilize the host ubiquitylation system to bypass the infected host immune system (see Refs. 7 and 8 for reviews).

Ubiquitylation consists of the attachment of one (monoubiquitylation) or more (multiubiquitylation of different lysine residues, or polyubiquitylation (*i.e.* the formation of a polyubiquitin chain)) ubiquitin moieties to a target protein via the formation of an isopeptide bond between the C-terminal diglycine motif of ubiquitin and a lysine in the target protein. The entire process requires the sequential intervention of three families of enzymes, namely E1 ubiquitin-activating enzymes, E2 ubiquitin-conjugating enzymes, and E3 ubiquitin ligases, involved in specific substrate recognition (see Refs. 1, 9, and 10 for reviews). In *P. falciparum*, previous *in silico* studies identified four predicted sources of ubiquitin moieties. The polyubiquitin gene PFL0585w contains five conserved ubiquitin repeats (9, 10). The two ubiquitin fusion proteins PfUB_{S27a} and PfUB_{L40} (PF14_0027 and PF13_0346, respectively) contain a ubiquitin moiety at their N-terminal side (10). More recently, one conserved ubiquitin domain was identified in PF08_0067 and is believed to be part of an endoplasmic reticulum-associated protein degradation (ERAD)³-like pathway (11). In addition to these four genes encoding ubiquitins, more than 100 proteins involved in the ubiquitylation system were identified *in silico* (10) (*i.e.* about 2% of the total protein-coding genes of *P. falciparum*). By contrast, only a few substrates for ubiquitylation have been identified in *P. falciparum*, including actin (12) and

^{*} This work was supported by University of California, Riverside, start-up funds (to K. L. R.).

^[S] The on-line version of this article (available at <http://www.jbc.org>) contains supplemental Tables S1–S5 and Fig. S1.

¹ Both authors contributed equally to this work.

² To whom correspondence should be addressed: Dept. of Cell Biology and Neuroscience, University of California, 900 University Ave., Riverside, CA 92521. Tel.: 951-827-5422; Fax: 951-827-3087; E-mail: karine.leroch@ucr.edu.

³ The abbreviations used are: ERAD, endoplasmic reticulum-associated protein degradation; NEM, *N*-ethylmaleimide; MudPIT, multidimensional protein identification technology; IP, immunoprecipitation; SUMO, small ubiquitin-like modifier; UB, ubiquitin.

the histone protein H2B (13). The quickly reversible character of ubiquitylation (intervention of deubiquitinases) and the rapid degradation of polyubiquitylated proteins (proteasome) render the isolation and analysis of ubiquitylated proteins challenging.

Various methods can be used to identify ubiquitylated proteins both *in silico* (14, 15) and experimentally (16–20), including immunoprecipitation of ubiquitylated proteins coupled to mass spectrometry analysis. In human, specific precipitation of ubiquitin-conjugated proteins identified 345 substrates for ubiquitylation (21). Here, we explore the *P. falciparum* ubiquitome (*i.e.* all of the proteins that are targets for ubiquitylation) using a combination of immunofluorescent localization of ubiquitin conjugates, detection of ubiquitylating activities of various parasite extracts, *in silico* prediction of ubiquitin targets genome-wide using the previously published algorithms *UbiPred* (14) and *UbiPred* (15), and immunoprecipitation of ubiquitin conjugates followed by immunoprecipitates analysis using multidimensional protein identification technology (MudPIT). The application of these techniques to the analysis of the *P. falciparum* ubiquitome during its asexual cell cycle permitted the discovery of unknown features. We found that more than half of the parasite's proteome represents possible targets for ubiquitylation. Nearly 100 of these targets were confirmed by MudPIT analysis. The data set contains a variety of parasite-specific proteins that are crucial for the parasite's metabolism and survival, such as the hemoglobinase plasmepsin II. The schizont stage was found to contain the largest number of ubiquitylated proteins, whereas the ring stage contained the least. This observation is consistent with the parasite's reduction in size and activity before maturation into invasive merozoites. Finally, we found evidence of heterologous mixed modifications, SUMO/UB, of the same substrate. Such modifications are believed to target sumoylated proteins to the proteasome for degradation. The biological implications of these findings are discussed.

EXPERIMENTAL PROCEDURES

Parasite Strain and Culture Conditions—Sorbitol-synchronized *P. falciparum* parasite strain 3D7 was cultured in human erythrocytes according to previously described protocols (22–24). For each experiment, cultures were harvested 48 h after the first sorbitol treatment (ring stage) and after 18 and 36 h (trophozoite and schizont morphological stages, respectively, monitored by Giemsa staining).

Ubiquitylation Assays—Parasite protein extracts were freshly prepared before each ubiquitylation assay. $2\text{--}5 \times 10^9$ parasites were extracted by 0.15% saponin lysis of red blood cells (15 min of incubation on ice) followed by three washes in ice-cold PBS supplemented with 2 mM PMSF. After 15 min of incubation on ice, the parasite pellet was resuspended in 1 ml of ice-cold cytoplasmic lysis buffer (20 mM HEPES, pH 7.9, 10 mM KCl, 1 mM EDTA, 1 mM EGTA, 1 mM DTT, 0.65% Igepal[®], 0.5 mM PMSF, Roche Complete mini EDTA-free mixture protease inhibitor) and left on ice for an additional 5 min. After 10 min of centrifugation at 4 °C and $1500 \times g$, the supernatant was collected (cytoplasmic protein extract), and the pelleted nuclei were lysed in 100 μ l of nuclei lysis buffer (20 mM HEPES, pH 7.9,

0.1 mM NaCl, 0.1 mM EDTA, 0.1 mM EGTA, 1.5 mM MgCl₂, 1 mM DTT, 25% glycerol, 1 mM PMSF, Roche Complete mini EDTA-free mixture protease inhibitor) for 20 min at 4 °C under vigorous shaking. The nuclear protein extract was then cleared by centrifugation at 4 °C and $6000 \times g$ for 10 min and combined with the cytoplasmic extract. Protein concentrations were measured by a Bradford assay (25).

Fresh (*i.e.* prepared the same day and never frozen) protein extracts were used to perform ubiquitylation assays according to a modified previously published protocol (26). 16.5 μ l of protein extract were mixed on ice with 18.5 μ l of ubiquitylation reaction mix (20 mM HEPES, pH 7.9, 1.5 mM DTT, 1 \times Energy Regeneration Solution (Boston Biochem), 5 μ g of biotinylated ubiquitin (Boston Biochem), and 20 μ g of native ubiquitin (Boston Biochem) and incubated at 30 °C under gentle agitation. After 2 h of incubation, the reaction was mixed with Laemmli buffer (27), run on a 10% SDS-PAGE, and transferred onto a PVDF membrane. After 2 h of incubation with streptavidin proteins coupled to horseradish peroxidase (Jackson ImmunoResearch Laboratories, Inc.), the presence of incorporated biotin-ubiquitin was revealed by electroluminescence (Pierce ECL Western blotting substrate).

Immunofluorescent Localization of Ubiquitylated Proteins—Immunofluorescence detection of ubiquitylated proteins was performed according to a modified version of a previously described protocol (28). Infected red blood cells were washed once with PBS, and an aliquot was resuspended in 300–400 volumes of PBS containing 1% BSA (w/v). 30- μ l aliquots of cell suspension were spotted on the surface of a depression slide and completely air-dried. The cells were then fixed for 10 min at room temperature with 4% paraformaldehyde in PBS. After rinsing the slide once with PBS, the cells were blocked with 1% BSA in PBS (w/v) for 30 min at room temperature in a humidified chamber. The liquid was then removed, and the slide was incubated with a 1:250 dilution of anti-conjugated ubiquitin antibody (clone FK2, Enzo[®] Life Sciences) in solution with 1% BSA, PBS (w/v) for 2 h at room temperature in a humidified chamber. After liquid removal and three washes with PBS for 5 min, the slide was incubated with a 1:250 dilution of secondary antibody (Texas Red[®]-X goat anti-mouse IgG, Invitrogen) in solution with 1% BSA, PBS (w/v) for 1 h at room temperature in a humidified chamber. After liquid removal and three washes with PBS for 5 min, nuclei were stained with DAPI (100 ng/ml) for 5 min. The slide was then carefully washed three times for 5 min with PBS. The slide was finally mounted with slow fade mounting medium (Fluoromount-G, Southern Biotech), and images were viewed with a fluorescence microscope within 72 h of preparing the slide. Images were prepared and mounted using the software ImageJ (National Institutes of Health, Bethesda, MD).

In Silico Identification of Putative Targets for Ubiquitylation—The complete set of 5446 translated coding sequences for *P. falciparum* was downloaded from PlasmoDB version 6.5 and analyzed for the presence of putative ubiquitylation sites using *UbiPred* (14) and *UbiPred* (15). Predictions with *UbiPred* were classified by level of confidence, from low (score ranging from 0.62 to 0.69) to medium (score ranging from 0.70 to 0.84) to high (score equal to or higher than 0.85), according to the soft-

Ubiquitylation in *P. falciparum*

ware instructions. With regard to the predictions made with *UbiPred*, proteins were considered potentially ubiquitylated with high confidence when prediction scores were equal to at least 0.85 (15).

Immunoprecipitation of Ubiquitylated Proteins—Protein ubiquitylation leads to the rapid degradation of the target protein by the proteasome, which is a major obstacle to the isolation and analysis of ubiquitylated proteins. To prevent the degradation of ubiquitylated proteins in the sample, parasite cultures were treated with 400 nM proteasome inhibitor MG132 (EMD Chemicals Inc.) 6 h before harvest. In addition, ubiquitin moieties are rapidly removed *in vivo* by deubiquitylating enzymes. To ensure maximum detection of targets for ubiquitylation, all reagents were supplemented with 20 mM *N*-ethylmaleimide (NEM), 2 mM PMSF, and Complete mini EDTA-free protease inhibitor mixture (Roche Applied Science). Cultures were harvested by 5 min of centrifugation at $800 \times g$ and 4°C , followed by three washes in PBS supplemented with NEM, PMSF, and anti-protease mixture. Parasites were extracted with 0.15% (w/v) saponin (in PBS) for 15 min on ice. Cells were pelleted by centrifugation for 10 min at $3200 \times g$ and 4°C and washed with PBS (supplemented with NEM, PMSF, and anti-protease mixture) until the supernatant came out clear. Parasite pellets were then flash-frozen and stored at -80°C until immunoprecipitation.

Parasites were thawed in immunoprecipitation buffer (0.5% Triton X-100, 50 mM Tris-HCl, pH 7.5, 300 mM NaCl, 20 mM NEM, 0.5 mM EDTA, 2 mM PMSF, Roche Complete mini EDTA-free protease inhibitor mixture) and lysed by six strokes of sonication (10 s each) on a Fisher dismembrator model 100 set to power $2\frac{1}{2}$. Lysates were cleared by 15 min of centrifugation at $13,000 \times g$ and 4°C and incubated with washed agarose A beads (Invitrogen) for 1 h at 4°C under constant agitation. After 10 min of centrifugation at $13,000 \times g$ and 4°C , the supernatant was incubated with anti-conjugated ubiquitin mouse IgG₁ (clone FK2 that does not react with free ubiquitin, Enzo Life Sciences) overnight at 4°C . In parallel, negative control samples were left without antibody (beads only). The conjugates and the negative control samples were then incubated with washed agarose A beads for 2 h at 4°C . The beads were collected by 30 s of centrifugation at $4000 \times g$, washed three times in immunoprecipitation buffer, and eluted with Laemmli buffer. Immunoprecipitates were analyzed by 12% SDS-PAGE, transfer on PVDF membrane, and incubation with a rabbit anti-ubiquitin IgG (Millipore) followed by immunodetection with a goat anti-rabbit IgG coupled to horseradish peroxidase (Millipore) and revelation by electroluminescence (Pierce ECL Western blotting substrate). Alternatively, immunoprecipitated proteins and negative controls were eluted three times from the beads with 50 μl of elution buffer (50 mM Tris-HCl, pH 6.8, 100 mM DTT, 2% SDS) before MudPIT analysis.

Immunoprecipitation of Plasmepsin II, Plasmepsin I, and Plasmepsin IV and Anti-ubiquitin Western Blot—Asynchronous cultures of parasites were treated with 400 nM MG132 (EMD Chemicals Inc.) 6 h before harvest. Cultures were harvested by 5 min of centrifugation at $800 \times g$ and 4°C , followed by three washes in PBS supplemented with NEM (20 mM), PMSF (2 mM), and complete mini EDTA-free protease inhibi-

tor mixture (Roche Applied Science). Parasites were extracted with 0.15% (w/v) saponin for 15 min on ice. Cells were pelleted by centrifugation for 10 min at $3200 \times g$ and 4°C and washed with PBS supplemented with NEM, PMSF, and anti-protease mixture until the supernatant came out clear. Parasite pellets were then flash-frozen and stored at -80°C until immunoprecipitation. Parasites were thawed in immunoprecipitation buffer and lysed by six strokes of sonication (10 s each) on a Fisher dismembrator model 100 set to power $2\frac{1}{2}$. Lysates were cleared by 15 min of centrifugation at $13,000 \times g$ and 4°C and incubated with washed PureProteomeTM magnetic protein A beads (Millipore) for 2 h at 4°C under constant agitation. Samples were then settled on a magnetic rack, and the supernatant was transferred to a fresh tube. The desired antibody was added to the tube and incubated overnight at 4°C under constant agitation. The conjugates were then incubated overnight with washed PureProteomeTM magnetic protein A beads at 4°C and constant agitation. Samples were then settled on a magnetic rack, and the supernatant was removed. The beads were then washed three times in immunoprecipitation buffer and eluted with Laemmli buffer. The immunoprecipitates were resolved by SDS-PAGE and transferred on PVDF membrane. Ubiquitylation was detected using a rabbit anti-ubiquitin IgG (Millipore) followed by immunodetection with a goat anti-rabbit IgG coupled to horseradish peroxidase (Millipore) and revelation by electroluminescence (ECL reagent, Pierce). Antibodies anti-plasmepsin I, II, and IV were obtained from the MR4, deposited by D.E. Goldberg (30–32) (accession numbers MRA-66, MRA-813A, and MRA-814A, respectively).

MudPIT Analysis of Immunoprecipitated Proteins—Immunoprecipitated proteins were TCA-precipitated, and the pellets were solubilized in 100 mM Tris-HCl, pH 8.5, and 8 M urea; tris(2-carboxylethyl)-phosphine hydrochloride (Pierce) and chloroacetamide (Sigma) were added to a final concentration of 5 and 10 mM, respectively. Protein suspensions were digested overnight at 37°C using endoproteinase Lys-C at 1:50 (w/w) (Roche Applied Science). Samples were brought to a final concentration of 2 M urea and 2 mM CaCl₂ before performing a second overnight digestion at 37°C using trypsin (Promega) at 1:100 (w/w). Formic acid (5% final) was added to stop the reactions. Samples were loaded on split triple-phase fused silica microcapillary columns (33) and placed in line with an Eksigent NanoLC 2D system. Full MS spectra were recorded on the peptides over a 400–1700 *m/z* range in the Orbitrap at 60,000 resolution, followed by fragmentation in the ion trap (at 35% collision energy) on the first to fifth most intense ions selected from the full MS spectrum with dynamic exclusion enabled for 90 s (34). A total of three, three, four, and seven technical replicates were acquired for the ring, trophozoite, schizont, and negative control samples, respectively.

MudPIT Data Analysis—RAW files were extracted into ms2 file format (35) using RAW_Xtract version 1.0 (36). MS/MS spectra were searched using SEQUEST version 27 (revision 9) (37) with a peptide mass tolerance of 50 ppm and searched against a protein database combining non-redundant 5439 *P. falciparum* (PlasmoDB release 5.5) and 30,552 human proteins (NCBI 2008-03-04 release) as well as 162 usual contaminants, such as human keratins, IgGs, and proteolytic enzymes.

To estimate false discovery rates, each protein sequence was randomized (keeping the same amino acid composition and length), and the resulting “shuffled” sequences were added to the database used for the SEQUEST searches, for a total search space of 72,306 amino acid sequences. To account for alkylation by chloroacetamide, +57 Da was added statically to cysteine residues for all searches. Peptide/spectrum matches were sorted, selected, and compared using DTASelect/CONTRAST (38). Peptides had to be full tryptic and at least 7 amino acids long, with a ΔCn cut-off of 0.08 and XCorr minima of 1.8, 2.0, and 3.0 for singly, doubly, and triply charged spectra. Proteins had to be detected by two such peptides or one peptide with two spectra in each run. NSAF version 7, an in-house developed software, was used to create the final report on all non-redundant proteins detected across the different MudPIT runs and calculate false discovery rates, which were on average 0.4 ± 0.3 and $0.7 \pm 0.4\%$ at the spectral and protein levels, respectively. Protein abundance was evaluated according to their normalized spectral abundance factors, calculated as the spectral count relative to the length of a given protein normalized by the sum of the relative spectral counts in the sample (34). We used the open source software package “plgem” (written in R and maintained by the BioConductor project) to establish some statistical significance on this data set (39). Briefly, the runs with the most replicates (negative controls) were used to fit a power law global error model on the mean *versus* S.D. plots. Then STN ratios against control as a base line were calculated using observed mean values and PLGEM-calculated S.D. values as follows.

$$\text{STN} = \frac{\text{ObsMean}_{\text{Stage}} - \text{ObsMean}_{\text{Control}}}{\text{CalcS.D.}_{\text{Stage}} + \text{CalcS.D.}_{\text{Control}}} \quad (\text{Eq. 1})$$

Finally, a series of random resampled STN ratios were computed to calculate significance thresholds (*p* values) of PLGEM-based STN values (supplemental Table S2). Proteins not detected in negative controls or with *p* values of ≤ 0.05 in at least one of the three stages examined were considered potential ubiquitylated conjugates (supplemental Table S2, first group of 73 *Plasmodium* proteins). The entire MS/MS data set was queried for the presence of lysines modified by 114.04 Da (“ubiquitin marks”) on the 49 proteins with significant *p* values, as described previously (40).

RESULTS

Ubiquitylation in *P. falciparum* Erythrocytic Stages—The *P. falciparum* genome contains more than 100 genes that are potentially encoding the components of the ubiquitylation system, including four sources of ubiquitin (PFL0585w, PF14_0027, PF13_0346, and PF08_0067), eight E1 enzymes (with various specificities for ubiquitin and ubiquitin-like moieties), 14 E2 enzymes, more than 50 E3 ubiquitin ligases, and about 30 deubiquitinases (10). To experimentally confirm the presence of an active ubiquitylation system during the asexual cell cycle of *P. falciparum*, fresh (same day) protein extracts were prepared from parasites harvested at ring, trophozoite, and schizont stages and tested for the presence of endogenous ubiquitylating activity (Fig. 1A). Ubiquityla-

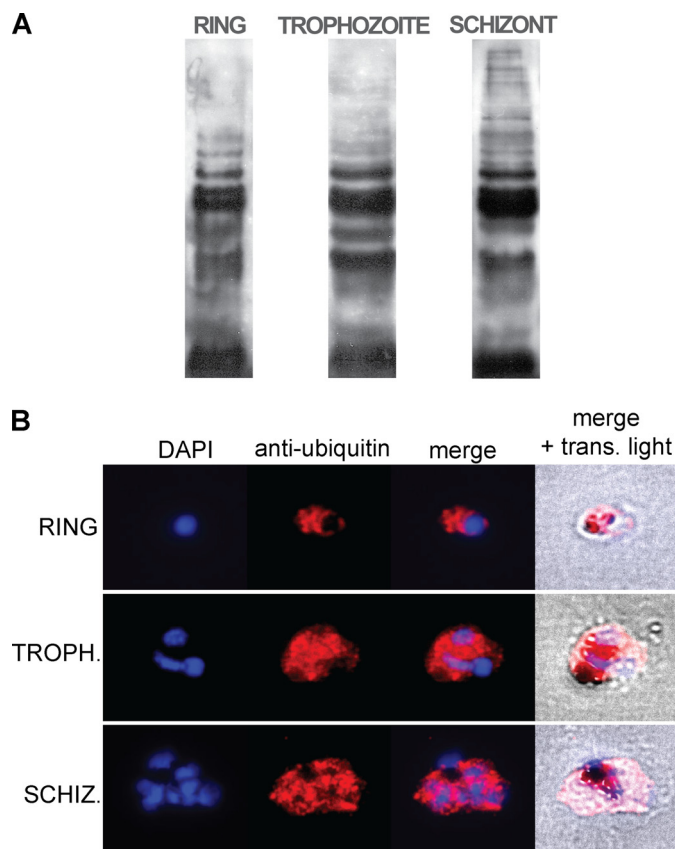


FIGURE 1. Ubiquitylation in *P. falciparum* at ring, trophozoite, and schizont stages. *A*, *in vitro* ubiquitylation activity of the parasite's protein extracts prepared at different morphological stages. Ubiquitylation assays were performed in the presence of biotin-ubiquitin and revealed by Western blot streptavidin-HRP with electrochemiluminescence detection. The presence of multiple bands reveals the presence of various biotin-ubiquitin conjugates. *B*, immunofluorescent *in situ* localization of ubiquitin conjugates in parasites at their ring, trophozoite (*TROPH.*), or schizont (*SCHIZ.*) stages. The parasites were visualized under transmitted (*trans.*) light, their nuclei were stained with DAPI (*blue*), and the ubiquitin conjugates were visualized in *red*. Ubiquitin conjugates are present at all investigated stages.

tion activity was detected in all three morphological stages of the parasite.

We further investigated the localization of ubiquitin conjugates in intraerythrocytic parasites by immunofluorescence microscopy using an anti-ubiquitin antibody that does not react with free ubiquitin (which minimizes eventual background due to the intracellular pool of free ubiquitin). Results are shown in Fig. 1*B*. At all stages, ubiquitin conjugates are detected in abundance in the entire cell. This pattern is consistent with the fact that ubiquitylation is usually found in both the cytoplasm and the nucleus. In addition, localized intense spots of fluorescence can be observed, consistent with the presence of ubiquitin conjugates in the parasite's vesicles. These results confirm the presence of a functional ubiquitylation system in all asexual stages of *P. falciparum*.

***In Silico* Identification of Putative Targets for Ubiquitylation**—We explored *in silico* the ubiquitome of *P. falciparum*. We used the algorithm *UbPred* to identify the proteins among the 5446 translated protein-coding sequences that contain favorable ubiquitylation sites (14). Three different cut-offs were used to classify the results: (i) all identified proteins (low to high confidence), (ii) proteins identified with medium to high confidence,

Ubiquitylation in *P. falciparum*

TABLE 1
Ubiquitin target predictions by *UbPred* (14)

Organism	Confidence level	Number of proteins	Percentage of the total proteome	Average number of sites/protein
<i>P. falciparum</i>	Low to high	5036	92.5	18.7
	Medium to high	4446	81.6	14.6
	High	3516	64.6	8.7
<i>S. cerevisiae</i>	Low to high	5258	89.3	7.9
	Medium to high	4470	76.0	6.0
	High	3059	52.0	4.1
<i>A. thaliana</i>	Low to high	42,953	82.9	5.6
	Medium to high	34,834	67.2	4.3
	High	20,214	39.0	3.1

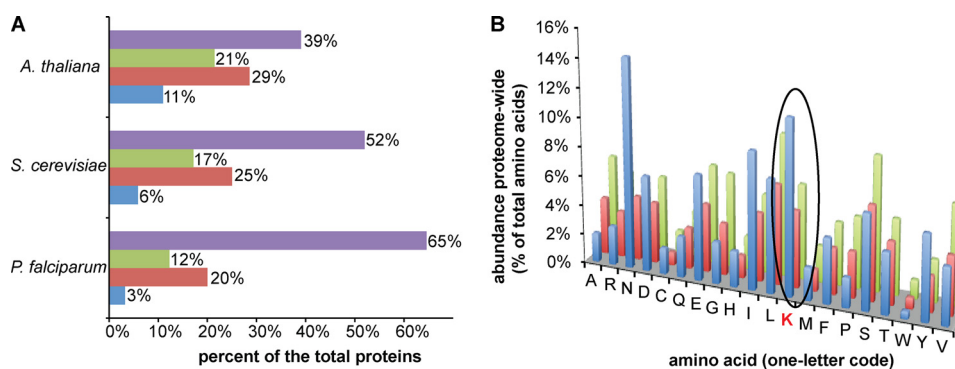


FIGURE 2. Comparison of proteomes for *P. falciparum*, *S. cerevisiae*, and *A. thaliana*. A, portion of the total proteome that, according to the *UbPred* algorithm, is not a target for ubiquitylation (blue bars) or a target for ubiquitylation according to *UbPred* predictions made with low (red bars), medium (green bars), or high confidence (purple bars). The large majority of *P. falciparum* proteins are confident putative targets for ubiquitylation. B, amino acid content in *P. falciparum* (blue bars), *S. cerevisiae* (red bars), and *A. thaliana* (green bars). The *P. falciparum* proteome contains a higher proportion of lysines than *S. cerevisiae* and *A. thaliana*.

and (iii) highly confident results only (see “Experimental Procedures” for more details). Results are summarized in Table 1. A total of 5036 proteins were predicted to contain ubiquitylation sites, 3516 of them with a high confidence level (i.e. ~65% of the input data set; Fig. 2A). This predicted abundance of targets for ubiquitylation is slightly higher than the predictions made for *Saccharomyces cerevisiae*, for which we found 52% of its proteome identified by *UbPred* with high confidence (*S. cerevisiae* data sets were used to train and test the accuracy of the algorithm). When the same algorithm was applied to the *Arabidopsis thaliana* proteome, only 39% of the total proteins were highly confident targets for ubiquitylation. In addition, the average number of ubiquitylation sites per protein is much higher in *P. falciparum* (Table 1). Following the same trend, lysine is the second most abundant amino acid in the *P. falciparum* proteome, with a frequency close to 12%, about double the frequencies observed in *S. cerevisiae* and *A. thaliana* (i.e. 5 and 6%, respectively) (Fig. 2B).

Slightly different results were obtained using *UbiPred*; 2077 proteins were predicted as ubiquitylated with high confidence (i.e. about 38% of the total proteome). This discrepancy might find its origin in the different data sets used to train the predicting algorithms. Both *UbPred* and *UbiPred* were built using ubiquitylated proteins as positive trainers. The negative data sets (non-ubiquitylated sites), however, were chosen differently; verified non-ubiquitylated proteins were used for the training of *UbPred*, whereas putative non-ubiquitylated sites were used to train *UbiPred*. As a consequence, the likelihood of false negatives is higher for results generated with *UbiPred*, consistent with a lower number of predicted targets for ubiquitylation.

The overlap between *UbPred* and *UbiPred* predictions consisted of 1332 proteins. Altogether, we identified a total of 4261 highly confident putative targets for ubiquitylation using *UbPred* and *UbiPred* in combination (~78% of the parasite’s proteome; see supplemental Table S1 for a complete list). The high lysine content of the parasite’s proteins and the relative abundance of predicted ubiquitin targets may indicate major roles for ubiquitylation in the biology of *P. falciparum*.

We examined in more details the cellular localization of the 4261 highly confident ubiquitin targets identified with *UbPred* and *UbiPred* (used in combination). We found 299 of them contain an apicoplast-targeting signal according to the plasmoAP rules (41, 42), 233 and 154 contain a PEXEL (43, 44) or HT (45) signal, respectively, and are targeted to the human host erythrocyte membrane, and 1288 have one or more transmembrane domains (46) (data queries made on PlasmoDB version 6.5). These values do not represent any significant enrichment of ubiquitylated proteins according to the cellular compartment.

MudPIT Identification of Ubiquitin Conjugates in *P. falciparum* Asexual Stages—Protein extracts were prepared from *P. falciparum* cultures harvested at ring, trophozoite, or schizont stage. Ubiquitin conjugates were then immunoprecipitated with an anti-ubiquitin antibody that does not recognize free ubiquitin (see “Experimental Procedures”) and visualized by anti-ubiquitin Western blot. We tested the immunoprecipitation procedure on an asynchronous population and confirmed that the antibody selectively enriches the sample in ubiquitin conjugates and does not precipitate free ubiquitin (Fig. 3A). The procedure was performed on stage-specific

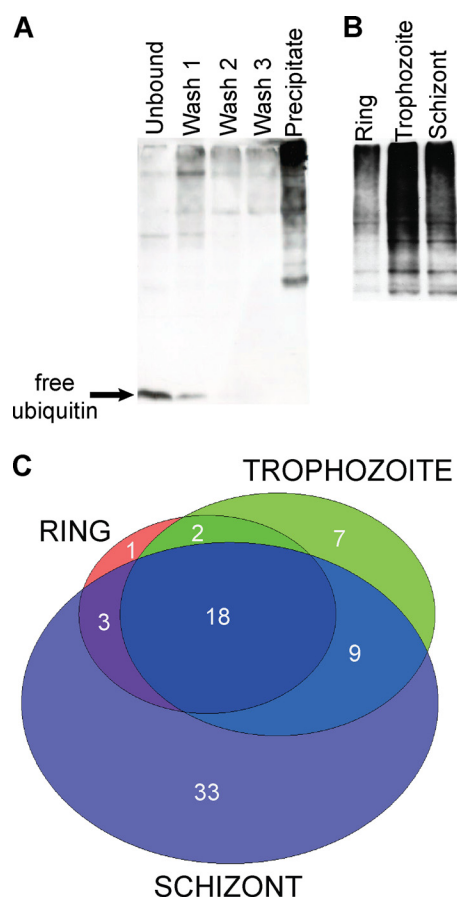


FIGURE 3. Selective immunoprecipitation and MudPIT identification of ubiquitin conjugates. *A*, antibody performances were tested on an asynchronous population of *P. falciparum* during its asexual cycle. The sample was first incubated with anti-ubiquitin antibody and then agarose beads. Proteins that were not captured by the antibody (unbound) were removed by centrifugation. The beads with antibody-ubiquitylated protein conjugates were washed three times (*Wash 1* to *Wash 3*) before the elution of specifically bound ubiquitylated proteins (*Precipitate*). Our results show a significant enrichment in ubiquitin conjugates in the immunoprecipitate without the presence of free ubiquitin. *B*, ubiquitin conjugate content in 10 μ l of immunoprecipitated proteins for rings, trophozoites, and schizonts. *C*, Venn diagram representing the number of different ubiquitin conjugates identified by MudPIT in each morphological stage.

extract. We found that all asexual intraerythrocytic stages contain ubiquitylated proteins (Fig. 3*B*).

The immunoprecipitated ubiquitin conjugates were further analyzed by MudPIT (see "Experimental Procedures"). A total of 437 proteins were detected from the anti-ubiquitin immunoprecipitated samples (supplemental Table S2). To increase the confidence of our analysis, we rejected all of the proteins that were not significantly enriched in the ubiquitin immunoprecipitations compared with samples precipitated in the absence of specific antibody (see "Experimental Procedures"). This method minimizes the possible number of false positives. The counterpart is nonetheless a higher rate of false negatives because proteins that precipitate nonspecifically in the absence of anti-ubiquitin antibody can still be conjugated to ubiquitin. Using this filter, we find 73 *Plasmodium* proteins, \sim 1.3% of the translated genome, that were specifically detected in the ubiquitin immunoprecipitations, 24 of them with low spectral counts. For comparison, previous works using similar technique (same antibody and same denaturing conditions) identi-

TABLE 2
Ubiquitin marks on ubiquitin itself found in *P. falciparum*

Lysine	Number of spectra found in MudPIT ^a	Score for UbPred predictions
Lys-6	8 (1.3%)	0.49
Lys-9	0	0.38
Lys-11	79 (13.3%)	0.54
Lys-27	0	0.38
Lys-29	0	0.56
Lys-48	477 (80.4%)	0.54
Lys-63	29 (4.9%)	0.62

^a Of 593 spectra obtained merging all runs.

fied 345 ubiquitin conjugates in human cells (21), \sim 1.7% of the translated genome, and 200 ubiquitin conjugates in *A. thaliana* (16), \sim 0.8% of the translated genome).

Ubiquitin conjugates were the most abundant in schizont stage, with 63 proteins identified (17 with low abundance) of 73 (Fig. 3*C*). A total of 33 proteins were specific to this stage (15 of them were found in the low abundance data set), and 18 were present at all stages (with various abundances), such as ubiquitin itself (gene PFL0585w), various ribosomal proteins, and parasite-specific proteases, such as plasmepsin II (gene PF14_0077). Among the 63 ubiquitin conjugates found at schizont stage, 50 are present in the highly confident *in silico*-predicted data set (see supplemental Tables S1 and S2), and 22 were predicted with low to medium confidence with at least one of the algorithms (including ubiquitin itself, gene PFL0585w; see supplemental Table S3). The 40 S ribosomal protein S15A (PFC0735w) was the only protein identified by neither *UbPred* nor *UbiPred*. Remarkably, ubiquitin (the polyubiquitin gene PFL0585w contains five ubiquitin repeats) was found in the low to medium confidence data set (supplemental Table S3). Ubiquitin contains seven lysine residues that can all serve for the extension of ubiquitin chains: Lys-6, Lys-11, Lys-27, Lys-29, Lys-33, Lys-48, and Lys-63. *UbPred* identified Lys-63 with low confidence, and *UbiPred* identified Lys-33 (low confidence, score = 0.53) and Lys-48 (medium/high confidence, score = 0.83). The scores for Lys-6, Lys-11, Lys-27, and Lys-29 were below threshold (data not shown). Our MudPIT analysis, nonetheless, found evidence of ubiquitylated Lys-6 and Lys-11 in the samples (supplemental Fig. S1). Spectra matching such modified peptides from the ubiquitin proteins represented 1.3 and 13.3% of the total spectral count, respectively (Table 2). Lys-48 and Lys-63 were also detected as modified (80.4 and 4.9% of the spectra). Lys-48 is the most abundant linkage usually found in eukaryotic cells and is involved in targeting ubiquitin-tagged substrates to the 26 S proteasome for degradation. The roles of Lys-6, Lys-11, Lys-27, Lys-29, and Lys-33 are still not understood (see Ref. 47 for a review). These results show that the linkages Lys-6, Lys-11, Lys-48, and Lys-63 (at least) exist in *P. falciparum*.

We found 24 and 36 ubiquitylated proteins in rings and trophozoites, respectively. The 60 S ribosomal protein L27a (PFF0885w) was found to be ubiquitylated at ring stage exclusively (5 spectral counts), and seven ubiquitin conjugates were trophozoite-specific (Table 3). Two of them are members of the ubiquitin/proteasome system in *P. falciparum* (10). UFD2 (PFD0265w) is a U-box ubiquitin ligase involved in the endoplasmic reticulum-associated protein degradation pathway

Ubiquitylation in *P. falciparum*

TABLE 3

Ubiquitin-conjugates specifically found in trophozoite stage

Gene names and product descriptions are given according to the GeneDB Web site unless specified otherwise. NA, not applicable.

Systematic name	Product description	Function within the ubiquitin/ proteasome system ^a	Spectral counts
PF10_0068	RNA-binding protein, putative	NA	5
PFB0715w	DNA-directed RNA polymerase II second largest subunit, putative	NA	2
PFD0265w	Pre-mRNA splicing factor, putative	Deubiquitinase (mov34)	3
PFF1415c	Heat shock DnaJ protein, putative	NA	2
MAL8P1.103	Conserved <i>Plasmodium</i> protein, unknown function	NA	2
PF08_0020	Ubiquitination-mediated degradation component, putative	UFD2 U-box ubiquitin ligase	6
PF14_0096	RNA-binding protein Bruno, putative (HoBo)	NA	2

^a Annotation proposed based on protein domain architecture (10).

(ERAD), and PFD0265w encodes a metallodeubiquitinase (Mov34) closely related to the PRP8 RNA splicing factor. PF10_0068, PFB0715w, and PF14_0096 are also involved in the metabolism of RNA.

Alternative Validation of Plasmepsin II as a Substrate for Ubiquitylation—The plasmepsin II is a cysteine protease that catalyzes the degradation of hemoglobin in the food vacuole of the human malaria parasite. After translation, the full-length protein (~51.4 kDa) is transported to the food vacuole, where a 124-amino acid-long N-terminal pro-domain is cleaved off to leave a 329-amino acid-long mature and functional plasmepsin II (Fig. 5A). We used the antibody Ab737 (MRA-66 (29)), targeted to the N-terminal portion of the mature protein, to immunoprecipitate both the full-length preprotein and the mature plasmepsin II (Fig. 4A). Ubiquitylations were revealed using an anti-ubiquitin antibody (Fig. 4B). The characteristic smear of ubiquitylated proteins at high molecular weights was observed in the total protein extract (Fig. 4, *input*) and in the flow-through (FT) of proteins from the IP. This smear was replaced by a characteristically banding pattern that indicates the presence of poly-/multiubiquitylation on the precursor and mature plasmepsin II. The signal indicating ubiquitylation was particularly strong on the mature form of the protein (Fig. 4C, *lanes 1–3*), in agreement with the predominance of mature plasmepsin II during the parasite's asexual cycle. We examined the sequence of the plasmepsin II with regard to our bioinformatic predictions of ubiquitylation sites (supplemental Table S4). We found 20 putative ubiquitylation sites when *UbiPred* and *UbiPred* are used in combination. Eight of these sites are present on the mature plasmepsin II.

Similar experiments were performed with regard to the hemoglobins plasmepsin I and IV. Specific antibodies were used to immunoprecipitate plasmepsin I and plasmepsin IV, respectively (see "Experimental Procedures"). Based on our mass spectrometry analysis, these two plasmepsins were found at relatively low levels in our samples and were not significantly enriched compared with the control (see supplemental Table S2). No evidence of specific ubiquitylation on the immunoprecipitated plasmepsins I and IV was detected using an anti-ubiquitin antibody (Fig. 4C) (data not shown). These results indicate that either these two plasmepsins are not ubiquitylated or their abundance is below detection threshold, consistent with our mass spectrometry analysis. Altogether, these observations confirm that the plasmepsin II is a genuine substrate for ubiquitylation and validate further our mass spectrometry analysis.

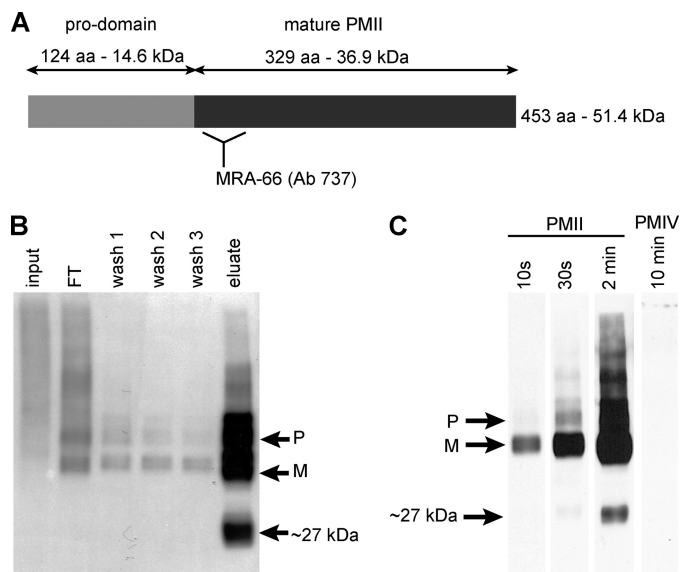


FIGURE 4. Alternative validation of plasmepsin II as a substrate for ubiquitylation. A, plasmepsin II (PMII) is translated into its 51.4-kDa pro-form and transported to the parasite's food vacuole, where it is processed into a 36.9-kDa mature and functional protease. The antibody MRA-66 (Ab737) recognizes the N-terminal side of the mature plasmepsin II and was used to immunoprecipitate the full-length and the mature plasmepsin II from protein extracts. B, anti-ubiquitin Western blot of the anti-plasmepsin II IP experiment (see "Experimental Procedures"). *Input*, full protein extract; *FT*, flow-through; *P*, precursor plasmepsin II; *M* = mature plasmepsin II. C, anti-ubiquitin Western blot of the anti-plasmepsin II IP experiment, with different exposure times, and of the anti-PMIV IP experiment. The ubiquitylated mature form of plasmepsin II is abundantly detected after 10 s of exposure. However, ubiquitylated PMIV is not detected after 10 min of exposure.

Functional Classification of the Ubiquitin Conjugates Identified by MudPIT—We examined in more detail the characteristics of the MudPIT data set. We classified the 73 proteins into 11 functional categories according to their annotation in PlasmoDB version 6.5 (Fig. 5). We found that 12% of the data set consisted of chaperon and other proteins involved in folding and that 11% of proteins were involved in translation (mostly ribosomal proteins), RNA metabolism (such as splicing factors), and ubiquitin-dependant metabolic processes (see supplemental Table S2). In human cells, proteins involved in translation/protein synthesis represent 18% of the immunoprecipitated ubiquitin conjugates (21). This value drops down to 4.5% in *A. thaliana* (16). Proteins involved in transcription represent 4% of the data set (*i.e.* twice as much as the proportion found in human cells (21) but half that of plants (16)). This group contained a subunit of the RNA polymerase II

(PFB0715w) and the putative ApiAP2 transcription factor PFF0200c that is mainly expressed and found ubiquitylated at schizont stage only (spectral count = 4).

Proteins involved in parasite-specific processes (invasion, hemoglobin metabolism, liver stage-specific) represent 8% of the data set. Remarkably, 11% of the data set contained proteins of the ubiquitin-proteasome system, an observation consistent with the fact that ubiquitin is covalently and sequentially attached to the various components of the ubiquitin machinery before being transferred on the targeted substrates (Table 4). Among them are components of the 26 S proteasome (PF08_0109, PF13_0063); the E2 enzyme PFC0255c, homolog to MMS2; and two ubiquitin ligases (the “E4” ligase UFD2 PF08_0020 and the zinc “RING” finger PF10_0046, homolog to the *A. thaliana* CIP8). Altogether, our observations showed that ubiquitin targets were involved in a wide array of biological processes in the parasite, including pathogenicity.

Relative Abundance of Ubiquitin Proteins in the Asexual Stages of *P. falciparum*—The abundance of each protein detected by MudPIT was estimated using the normalized spectral abundance factor (34). As expected, ubiquitin originated from mono- and polyubiquitin chains was by far the most abundant protein found in all samples (supplemental Table S2). The detected levels peaked at trophozoite stage (Fig. 6, solid line). We compared these abundances to the ubiquitin levels detected in a previous whole proteome analysis (48). In this study, Le Roch *et al.* showed that ubiquitin proteins are more abundant at ring and schizont stage than trophozoite stage (Fig. 6, dashed line). The discrepancies between our IP data and the ubiquitin levels of Le Roch *et al.* (48) can be explained by the fact that the antibody used in our immunoprecipitations does

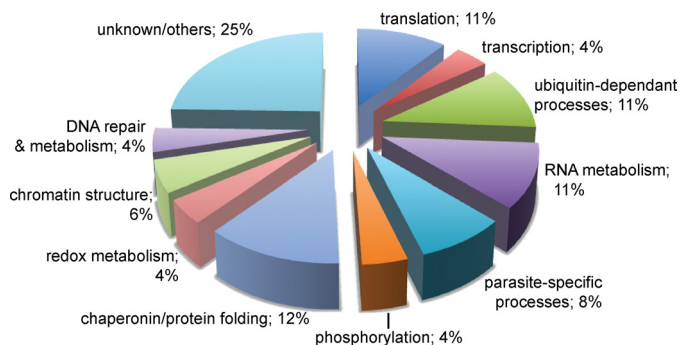


FIGURE 5. Functions of the ubiquitin targets identified by MudPIT. Ubiquitin conjugates were classified according to their known or suspected function and expressed as a percentage of the total ubiquitin conjugates.

TABLE 4

Components of the ubiquitin/proteasome system identified by immunoprecipitation coupled to MudPIT

Gene names and product descriptions are given according to the GeneDB Web site unless specified otherwise. NA, not applicable.

Gene name	Systematic name	Product description	Stage(s)	Spectral count(s) ^a
Polyubiquitin	PFL0585w	Polyubiquitin	Ring, trophozoite, schizont	266, 632, 265
MMS2 ^b	PFC0255c	Ubiquitin-conjugating enzyme E2, putative	Trophozoite, schizont	2, 8
UFD2	PF08_0020	Ubiquitination-mediated degradation component, putative (U-box ubiquitin ligase)	Trophozoite	6
CIP8	PF10_0046	E3 “RING” ubiquitin ligase, putative	Ring, trophozoite, schizont	2, 3, 2
NA	PF11_0142	Ubiquitin domain-containing protein	Trophozoite, schizont	6, 17
NA	PF08_0109	Proteasome subunit α type 5, putative	Trophozoite, schizont	2, 6
NA	PF13_0063	26 S proteasome-regulatory subunit 7, putative	Trophozoite, schizont	4, 4
SUMO	PFE0285c	Small ubiquitin-like modifier, putative	Ring, trophozoite, schizont	2, 3, 4

^a Average spectral count among all replicates with a positive count.

^b According to BLASTP results performed on the NCBI refseq protein database.

not recognize free ubiquitin. In this regard, the increased levels of total ubiquitin at ring and schizont stage in the whole proteome data set may be attributed to a higher pool of free ubiquitin at these stages. This hypothesis is consistent with a higher diversity of ubiquitin conjugates at schizont stage that appears dramatically reduced at ring stage.

Total Protein Levels Versus Ubiquitylated Protein Levels—We further compared our data set with total protein levels measured by Le Roch *et al.* (48) in their previous whole proteome analysis. Of the 73 ubiquitin conjugates that we specifically identified in the present work, 42 were present in the data set of Le Roch *et al.* (48) (supplemental Table S5).

In some instances, such as PFL1425w (γ subunit of T complex protein 1) at ring and schizont stages or PF11_0161 (falcipain 2b) at schizont stage, for example, no protein had been detected during the proteomic analysis, but ubiquitylated ones were identified in our data set (see supplemental Table S5). In these cases, because our samples were treated with the proteasome inhibitor MG132 for 6 h before harvest, it is likely that the detected conjugates are targeted to the proteasome for degradation. This hypothesis is consistent with various discrepancies observed by Le Roch *et al.* (48) between mRNA protein levels in a given stage and highlight the importance of post-transcriptional and post-translational regulations for the parasite's biology.

We more formally investigated the relationship between protein abundance in our IP samples and total protein abundance extracted from Le Roch *et al.* (48) (ring, trophozoite, and schizont stages) by measuring the Pearson product-moment correlation coefficient R^2 . R^2 was higher than 0.6 (strong positive association) for 11 of the considered proteins (of 41, not including ubiquitin). This observation indicates continuous ubiquitylation of these proteins across the different stages of the parasite, at various levels, and also suggests that both proteasome-dependant and -independent ubiquitylation events are involved.

DISCUSSION

The present study proposes more than 4200 putative ubiquitin substrates and validates $\sim 2\%$ of them for ubiquitylation during the intraerythrocytic cycle of the human malaria parasite *P. falciparum*. Ubiquitylated proteins were detected in all cellular compartments of the parasite, consistent with observations in other eukaryotes. Altogether, we found a high proportion of the proteome representing possible targets for

Ubiquitylation in *P. falciparum*

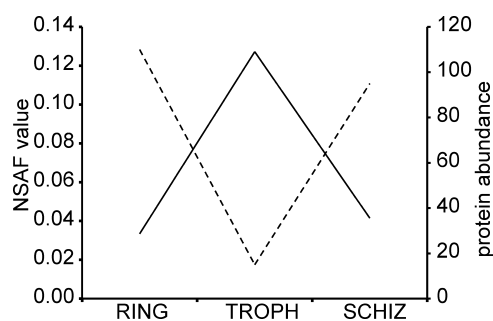


FIGURE 6. **Abundance of ubiquitin in IP samples versus total ubiquitin pool.** Ubiquitin abundance in immunoprecipitated samples was measured by the average normalized spectral abundance factor value observed at each asexual stage (solid curve). The total pool of ubiquitin in each stage has been quantified previously (48) (dashed curved). The Pearson product-moment coefficient of correlation between the two data sets equals -0.998 .

ubiquitylation across the various stages of the parasite's life cycle. This observation is consistent with a particularly high lysine content in the *P. falciparum* proteome that offers many possible anchor points for ubiquitin. In addition, these results represent other pieces of evidence that post-translational modifications in general and ubiquitylation in particular are major regulatory pathways in the malaria parasite. Most of the ubiquitin conjugates that we identified were found during the schizont stage, consistent with a reduction in size and activity of the parasite for maturation into the invasive merozoite. We nonetheless showed that a smaller number of proteins that ubiquitin conjugates were detected in the other intraerythrocytic stages. When coupled to previously published proteomic analysis (48), higher levels of ubiquitin are expected at ring and trophozoite stages, revealing a higher pool of free ubiquitin in these stages than in schizont stage. This observation highlights the importance of ubiquitylation events at the schizont stage before differentiation into the invasive merozoite. Given these elements, ubiquitylation events may be of major importance for merozoite differentiation.

The results obtained *in silico* using the two distinct algorithms *UbPred* and *UbiPred* show good overlap. The discrepancies observed between the two algorithms probably originate from their differences of conception. Both *UbPred* and *UbiPred* were built using positive (ubiquitylated) and negative (non-ubiquitylated sites) data sets, with an important difference in the choice of the negative data set. *UbPred* was trained to recognize non-ubiquitylated sites on *experimentally verified* non-ubiquitylated proteins. The negative data set for *UbiPred*, on the other hand, consisted of *putative* non-ubiquitylated sites more likely to contain more false negatives than the experimentally verified one. As a consequence, the likelihood of false negatives is higher for results generated with *UbiPred*, consistent with fewer predicted targets for ubiquitylation. In addition, we found that the two algorithms perform differently depending on the type of linkage that is considered. These differences probably have roots within the nature of training data sets. Less abundant linkages are more difficult to detect. *P. falciparum* seems to contain a relatively high proportion of K11 linkages, 13.3%. K11 linkages in humans are suspected of playing a key role in mitotic protein degradation (49). In *S. cerevisiae*, high levels of K11 linkages have been observed and are suspected to

be of major importance in ERAD of proteins (50). *Plasmodium* possesses a conventional ERAD system. In addition, there is growing evidence of an ERAD-like pathway that is involved in protein translocation to the parasite-specific plastid, namely the apicoplast (11, 51), the essentiality of which for the parasite's survival is clearly established (see Ref. 52 for a review). The potential importance of such linkages in *Plasmodium* (suggested by their abundance) could thus be major in terms of cell cycle progression, parasite survival, and virulence. When the levels of ubiquitylated proteins were compared with previously published levels of total proteins (48), we found that proteasome-dependent ubiquitylation may explain, in some instances, discrepancies between mRNA levels and protein levels (48). In other cases, it is likely that proteasome-independent ubiquitylations occur in the malaria parasite. Such post-translational modifications are known to be involved in protein targeting and regulation in eukaryotes.

From the technical point of view, our method is sensitive and accurate. Both the *Plasmodium* and the human databases were used to cross-match the detected peptides and specifically identify proteins based on their sequences. This step is indeed crucial, given that the red blood cell contains a wide range of proteins independently from *Plasmodium* infection (reviewed in Refs. 53 and 54). Our analysis, however, highlights the limits of the approach that was used to identify ubiquitin conjugates on a large scale. The main challenge is indeed to obtain a reliable negative control to exclude false positives while minimizing the number of false negatives; nonspecific interactions do not necessarily invalidate the specific ones. As is, we identified 73 *Plasmodium* ubiquitin conjugates together with 364 potential additional candidates. The rejection of these 364 candidates is directly linked to the base line drawn by the chosen negative control. The question of how to choose a good control to draw a *blank* base line receives, indeed, no perfect answer. Using various experimental strategies (*e.g.* protein capture via ubiquitin-binding domains) could provide a part of the solution by permitting a broader discovery of the various ubiquitin conjugates.

The 73 proteins in our data set of confident ubiquitin conjugates are involved in a variety of biological processes, such as translation. Many ribosomal proteins are ubiquitylated during the red blood cell cycle of *P. falciparum*. In human cells, the ribosomal subunits S3, S18, L23a, L24, and L28 were previously shown to be ubiquitylated (21, 55). Our results are consistent with a function for ubiquitylation in the quality control of ribosome biogenesis. Ribosome assembly, indeed, is a highly complex association of numerous and various proteins thus prone to misfolding and other maturation errors. The high proportion of ubiquitylated proteins in our data set may reflect this propensity to errors and the subsequent targeting to the proteasome after ubiquitin tagging. Another hypothesis is that ubiquitylation of ribosomal proteins plays a role in the regulation of translation, as shown previously in human cells (55).

Our data set also contained 11 proteins related to the ubiquitin/proteasome system itself. Because all interactions between ubiquitin and the enzymes catalyzing its transfer to various targets (including ultimately the proteasome) involve the formation of a covalent bond, the identification of a subset

of these enzymes is a validation of our data set. Most of the proteins that we identified are subunits of the proteasome. In addition, we also found one E2 ubiquitin-conjugating enzyme, two ubiquitin ligases, and the ubiquitin-like PFSUMO (PFE0285c). The existence of heterologous ubiquitin chains mixed with SUMO has been previously observed in other organisms (see Ref. 56 for a review) but has never been reported in *Plasmodium*. The proposed function of heterologous SUMO/UB chains is to target sumoylated proteins to the proteasome for degradation. Various SUMO targets were previously reported and indicated an important role of sumoylation in the parasite's biology (57). Among them, Issar *et al.* (57) identified several transcription and chromatin regulators, including the histone protein H4 (PF11_0061) that we also identified in our data set. Our results further suggest that the histone variant H2A.Z (and possibly H2A, H2B, and H3) is also a target for ubiquitylation. Such ubiquitylation has been observed previously in human and yeast and is possibly linked to gene activity (see Ref. 58 for a review). In addition, we also found a major subunit of the RNA polymerase II conjugated to ubiquitin at trophozoite stage (see supplemental Table S2). Such ubiquitylation was previously associated with transcriptional arrest in yeast (reviewed in Ref. 59 and 60) but was never observed in *Plasmodium*. Finally, we found that at least one of the few specific ApiAP2 transcription factors that are known in *Plasmodium*, PFF0200c, is ubiquitylated at schizont stage. Altogether, these data strongly indicate that ubiquitylation play an important role in regulating gene expression at the transcriptional level. A few proteins involved in the parasite's specific processes, such as the hemoglobinase plasmepsin II, were also identified (the ubiquitylation of plasmepsin II was further validated by immunodetection).

Our results provide the first general view of the *P. falciparum* ubiquitome and represent an important step toward the characterization of the ubiquitylation system in the parasite. This study identifies various new targets for ubiquitylation and provides numerous leads for investigating the malaria parasite's biology through post-translational modifications. On the whole, our observations strongly propose ubiquitination as a major regulator of various biological processes in *Plasmodium*, including gene expression and various parasite-specific metabolisms. The ubiquitin targets shown in the present work could therefore represent excellent objects of research for future development of anti-malarial drugs.

Acknowledgments—We thank P. Radivojac for providing a stand-alone version of UbPred for Windows® 32 bits and C.-W. Tung for running Ubipred. The following reagents were obtained through the MR4 as part of the BEI Resources Repository, NIAID, National Institutes of Health: *P. falciparum* 1C6-24, MRA-813A; *P. falciparum* anti-plasmepsin II rabbit antiserum 737 MRA-66; *P. falciparum* 13.9.2, MRA-814A, deposited by D. E. Goldberg.

REFERENCES

- Chung, D. W., Ponts, N., Cervantes, S., and Le Roch, K. G. (2009) *Mol. Biochem. Parasitol.* **168**, 123–134
- Petroski, M. D. (2008) *BMC Biochem.* **9**, S7–S7
- Berkers, C. R., and Ovaa, H. (2010) *Biochem. Soc. Trans.* **38**, 14–20
- Prudhomme, J., McDaniel, E., Ponts, N., Bertani, S., Fenical, W., Jensen, P., and Le Roch, K. (2008) *PLoS ONE* **3**, e2335
- Reynolds, J. M., El Bissati, K., Brandenburg, J., Günzl, A., and Mamoun, C. B. (2007) *BMC Clin. Pharmacol.* **7**, 13
- Lindenthal, C., Weich, N., Chia, Y. S., Heussler, V., and Klinkert, M. Q. (2005) *Parasitology* **131**, 37–44
- Edelmann, M. J., and Kessler, B. M. (2008) *Biochim. Biophys. Acta* **1782**, 809–816
- Spallek, T., Robatzek, S., and Göhre, V. (2009) *Cell. Microbiol.* **11**, 1425–1434
- Ponder, E. L., and Bogyo, M. (2007) *Eukaryotic Cell* **6**, 1943–1952
- Ponts, N., Yang, J., Chung, D. W., Prudhomme, J., Girke, T., Horrocks, P., and Le Roch, K. G. (2008) *PLoS ONE* **3**, e2386
- Spork, S., Hiss, J. A., Mandel, K., Sommer, M., Kooij, T. W., Chu, T., Schneider, G., Maier, U. G., and Przyborski, J. M. (2009) *Eukaryotic Cell* **8**, 1134–1145
- Field, S. J., Pinder, J. C., Clough, B., Dluzewski, A. R., Wilson, R. J., and Gratzer, W. B. (1993) *Cell Motil. Cytoskeleton* **25**, 43–48
- Trelle, M. B., Salcedo-Amaya, A. M., Cohen, A. M., Stunnenberg, H. G., and Jensen, O. N. (2009) *J. Proteome Res.* **8**, 3439–3450
- Radivojac, P., Vacic, V., Haynes, C., Cocklin, R. R., Mohan, A., Heyen, J. W., Goebel, M. G., and Iakoucheva, L. M. (2010) *Proteins* **78**, 365–380
- Tung, J., Primus, A., Bouley, A. J., Severson, T. F., Alberts, S. C., and Wray, G. A. (2009) *Nature* **460**, 388–391
- Manzano, C., Abraham, Z., López-Torrejón, G., and Del Pozo, J. C. (2008) *Plant Mol. Biol.* **68**, 145–158
- Tan, F., Lu, L., Cai, Y., Wang, J., Xie, Y., Wang, L., Gong, Y., Xu, B. E., Wu, J., Luo, Y., Qiang, B., Yuan, J., Sun, X., and Peng, X. (2008) *Proteomics* **8**, 2885–2896
- Hjerpe, R., Aillet, F., Lopitz-Otsoa, F., Lang, V., England, P., and Rodriguez, M. S. (2009) *EMBO Rep.* **10**, 1250–1258
- Tomlinson, E., Palaniyappan, N., Tooth, D., and Layfield, R. (2007) *Proteomics* **7**, 1016–1022
- Golebiowski, F., Tatham, M. H., Nakamura, A., and Hay, R. T. (2010) *Nat. Protoc.* **5**, 873–882
- Matsumoto, M., Hatakeyama, S., Oyamada, K., Oda, Y., Nishimura, T., and Nakayama, K. I. (2005) *Proteomics* **5**, 4145–4151
- Lambros, C., and Vanderberg, J. P. (1979) *J. Parasitol.* **65**, 418–420
- Le Roch, K. G., Zhou, Y., Blair, P. L., Grainger, M., Moch, J. K., Haynes, J. D., De La Vega, P., Holder, A. A., Batalov, S., Carucci, D. J., and Winzeler, E. A. (2003) *Science* **301**, 1503–1508
- Trager, W., and Jensen, J. B. (1976) *Science* **193**, 673–675
- Bradford, M. M. (1976) *Anal. Biochem.* **72**, 248–254
- Qin, F., Sakuma, Y., Tran, L. S., Maruyama, K., Kidokoro, S., Fujita, Y., Fujita, M., Umezawa, T., Sawano, Y., Miyazono, K., Tanokura, M., Shinozaki, K., and Yamaguchi-Shinozaki, K. (2008) *Plant Cell* **20**, 1693–1707
- Laemmli, U. K. (1970) *Nature* **227**, 680–685
- Tonkin, C. J., van Dooren, G. G., Spurck, T. P., Struck, N. S., Good, R. T., Handman, E., Cowman, A. F., and McFadden, G. I. (2004) *Mol. Biochem. Parasitol.* **137**, 13–21
- Francis, S. E., Sullivan, D. J., Jr., and Goldberg, D. E. (1997) *Annu. Rev. Microbiol.* **51**, 97–123
- Banerjee, R., Francis, S. E., and Goldberg, D. E. (2003) *Mol. Biochem. Parasitol.* **129**, 157–165
- Banerjee, R., Liu, J., Beatty, W., Pelosof, L., Klemba, M., and Goldberg, D. E. (2002) *Proc. Natl. Acad. Sci. U.S.A.* **99**, 990–995
- Francis, S. E., Banerjee, R., and Goldberg, D. E. (1997) *J. Biol. Chem.* **272**, 14961–14968
- McDonald, W. H., Ohi, R., Miyamoto, D. T., Mitchison, T. J., and Yates, J. R. (2002) *Int. J. Mass Spectrom.* **219**, 245–251
- Zhang, Y., Wen, Z., Washburn, M. P., and Florens, L. (2010) *Anal. Chem.* **82**, 2272–2281
- McDonald, W. H., Tabb, D. L., Sadygov, R. G., MacCoss, M. J., Venable, J., Graumann, J., Johnson, J. R., Cociorva, D., and Yates, J. R., 3rd (2004) *Rapid Commun. Mass Spectrom.* **18**, 2162–2168
- Venable, J. D., Dong, M. Q., Wohlschlegel, J., Dillin, A., and Yates, J. R. (2004) *Nat. Methods* **1**, 39–45
- Eng, J. K., McCormack, A. L., and Yates, J. R., 3rd (1994) *J. Am. Soc. Mass*

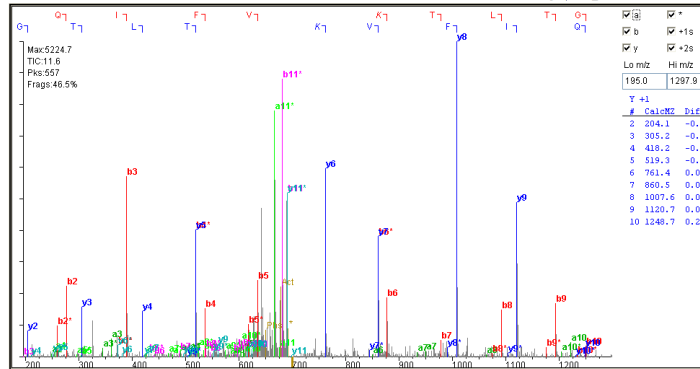
Ubiquitylation in *P. falciparum*

- Spectrom.* **5**, 976–989
38. Tabb, D. L., McDonald, W. H., and Yates, J. R., 3rd (2002) *J. Proteome Res.* **1**, 21–26
39. Pavelka, N., Fournier, M. L., Swanson, S. K., Pelizzola, M., Ricciardi-Castagnoli, P., Florens, L., and Washburn, M. P. (2008) *Mol. Cell Proteomics* **7**, 631–644
40. Xiang, Y., Takeo, S., Florens, L., Hughes, S. E., Huo, L. J., Gilliland, W. D., Swanson, S. K., Teeter, K., Schwartz, J. W., Washburn, M. P., Jaspersen, S. L., and Hawley, R. S. (2007) *PLoS Biol.* **5**, e323
41. Foth, B. J., Ralph, S. A., Tonkin, C. J., Struck, N. S., Fraunholz, M., Roos, D. S., Cowman, A. F., and McFadden, G. I. (2003) *Science* **299**, 705–708
42. Tonkin, C. J., Foth, B. J., Ralph, S. A., Struck, N., Cowman, A. F., and McFadden, G. I. (2008) *Proc. Natl. Acad. Sci. U.S.A.* **105**, 4781–4785
43. Marti, M., Baum, J., Rug, M., Tilley, L., and Cowman, A. F. (2005) *J. Cell Biol.* **171**, 587–592
44. Marti, M., Good, R. T., Rug, M., Knuepfer, E., and Cowman, A. F. (2004) *Science* **306**, 1930–1933
45. Hiller, N. L., Bhattacharjee, S., van Ooij, C., Liolios, K., Harrison, T., Lopez-Estraño, C., and Haldar, K. (2004) *Science* **306**, 1934–1937
46. Krogh, A., Larsson, B., von Heijne, G., and Sonnhammer, E. L. (2001) *J. Mol. Biol.* **305**, 567–580
47. Kirkpatrick, D. S., Denison, C., and Gygi, S. P. (2005) *Nat. Cell Biol.* **7**, 750–757
48. Le Roch, K. G., Johnson, J. R., Florens, L., Zhou, Y., Santrosyan, A., Grainger, M., Yan, S. F., Williamson, K. C., Holder, A. A., Carucci, D. J., Yates, J. R., 3rd, and Winzler, E. A. (2004) *Genome Res.* **14**, 2308–2318
49. Matsumoto, M. L., Wickliffe, K. E., Dong, K. C., Yu, C., Bosanac, I., Bustos, D., Phu, L., Kirkpatrick, D. S., Hymowitz, S. G., Rape, M., Kelley, R. F., and Dixit, V. M. (2010) *Mol. Cell* **39**, 477–484
50. Xu, P., Duong, D. M., Seyfried, N. T., Cheng, D., Xie, Y., Robert, J., Rush, J., Hochstrasser, M., Finley, D., and Peng, J. (2009) *Cell* **137**, 133–145
51. Sommer, M. S., Gould, S. B., Lehmann, P., Gruber, A., Przyborski, J. M., and Maier, U. G. (2007) *Mol. Biol. Evol.* **24**, 918–928
52. McFadden, G. I. (2011) *Protoplasma*, in press
53. D'Alessandro, A., Righetti, P. G., and Zolla, L. (2010) *J. Proteome Res.* **9**, 144–163
54. Goodman, S. R., Kurdia, A., Ammann, L., Kakhniashvili, D., and Daescu, O. (2007) *Exp. Biol. Med.* **232**, 1391–1408
55. Spence, J., Gali, R. R., Dittmar, G., Sherman, F., Karin, M., and Finley, D. (2000) *Cell* **102**, 67–76
56. Ikeda, F., and Dikic, I. (2008) *EMBO Rep.* **9**, 536–542
57. Issar, N., Roux, E., Mattei, D., and Scherf, A. (2008) *Cell. Microbiol.* **10**, 1999–2011
58. Weake, V. M., and Workman, J. L. (2008) *Mol. Cell* **29**, 653–663
59. Svejstrup, J. Q. (2007) *Trends Biochem. Sci.* **32**, 165–171
60. Daulny, A., and Tansey, W. P. (2009) *DNA Repair* **8**, 444–448

L	Locus	Description	Residue	Mass	Sequence Alignment	XCorr	Filename	ModCount	Copy Count
M	Modified	Difference							
L	psu PF13_0346	product=ubiquitin/ribosomal fusion protein uba52 homologue, putative							
L	psu PFL0585w								
M		1	15.995	<u>M</u> QIFVKT <u>L</u> TGK	3.8399	Pf_Schi-ub-36h_25ug_OT-60K_Ti_106.008141.008141.2		2	8
M		6	114.04	MQIFVKT <u>L</u> TGK	3.8399	Pf_Schi-ub-36h_25ug_OT-60K_Ti_106.008141.008141.2		2	8

1397.77 amu Pf_Schi-ub-36h_25ug_OT-60K_Ti_106.008141.xxxxx.2 db:/data1/proteomics/db/Pf_PlasmoDB_5.5_Hs_NCBI_2008-03-04_NR_wSHUFFLED_wNP.fasta

Rank	Sp	(M+H) ⁺	delCn	XCorr	Sp	Ions	Reference	Peptide
1	1	1395.76696	0.0000	3.8399	6.312	18/20	psuPF13_0346	-M#QIFVK-ILTKG*.I
2	5	1395.76359	0.3215	2.6052	3.316	12/18	psuPF14_0454	K.K*INQVLEK.I
3	2	1397.73502	0.3620	2.4499	2.939	14/20	psuMAL13P1.133	K.YIIM#ENTRIEK.I
4	41	1396.69686	0.3922	2.3340	2.658	12/22	SHUFFLED_gi21361937refNP_085044.2	R.YLLEACLAVGK.E
5	3	1395.76696	0.4030	2.2925	2.557	13/20	psuPF13_0346	-M#QIFVKILTKG*.I

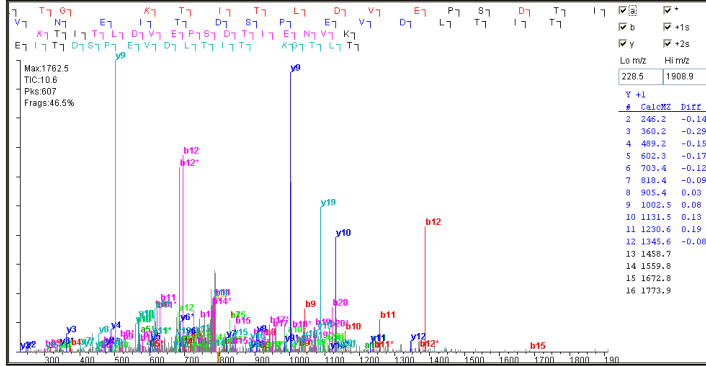


L Locus Description

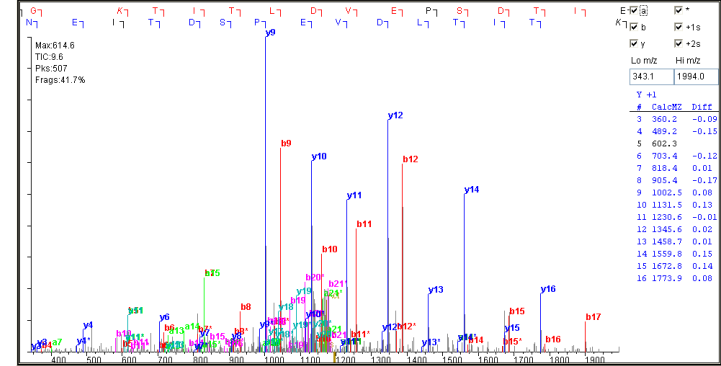
M	Residue Modified	Mass Difference	Sequence Alignment	XCorr	Filename	ModCount	Copy Count
L	psu PF13_0346	product=ubiquitin/ribosomal fusion protein uba52 homologue, putative					
L	psu PFL0585w						
M	11	114.04	TLTGK T ITLDVEPSDTIENVK	4.8302	Pf_Schi-ub-36h_25ug_OT-60K_Ti_308.010202.010202.3	1	39
M	11	114.04	TLTGK T ITLDVEPSDTIENVK	5.8461	Pf_Schi-ub-36h_25ug_OT-60K_Ti_208.009221.009221.2	1	40

2388.26 amu Pf_Schi-ub-36h_25ug_OT-60K_Ti_308.010202.xxxxx.3 db: /data1/proteomics/db/Pf_PlasmoDB_5.5_Hs_NCBI_2008-03-04_NR_wSHUFFLED_vNTP.fasta 2389.25 amu Pf_Schi-ub-36h_25ug_OT-60K_Ti_208.009221.xxxxx.2 db: /data1/proteomics/db/Pf_PlasmoDB_5.5_Hs_NCBI_2008-03-04_NR_wSHUFFLED_vNTP.fasta

Rank	Sp	(M+H) ⁺	deltCn	XCorr	Sp	Ions	Reference	Peptide
1	1	2388.25094	0.0000	4.8302	7969	34/80	psu PF13_0346	R.LTLGK* T ITLDVEPSDTIENVK.A
2	73	2387.14874	0.5448	2.1988	2564	22/80	SHUFFLED_gi21040334ref NP_612808.1	R.VENCIPFPK* F ARM#SPSPAAEK.N
3	97	2388.16175	0.5503	2.1719	2509	19/76	SHUFFLED_gi70608082ref NP_001002010.1	R.RPNMEFR* D VDSQALTAEK.L
4	41	2388.22666	0.5507	2.1703	2506	20/72	psu PFL0875w	R.DNIMTKINVENNICIELIK*.K
5	437	2388.27430	0.5528	2.1601	2485	16/80	gi62243658ref NP_055907.3	R.LSSANFTMVLGVQ#ELVAELRR.V



Rank	Sp	(M+H) ⁺	deltCn	XCorr	Sp	Ions	Reference	Peptide
1	1	2388.25094	0.0000	5.8461	9179	22/40	psu PF13_0346	R.LTLGK* T ITLDVEPSDTIENVK.A
2	3	2389.26481	0.5653	2.5412	2690	15/38	SHUFFLED_psu PF10_0340	R.CHEVITIDKSVISISLNIER*.V
3	24	2388.22666	0.5700	2.5138	2636	12/36	psu PFL0875w	R.DNIMTKINVENNICIELIK*.K
4	100	2389.16191	0.5741	2.4896	2589	10/36	SHUFFLED_gi11641255ref NP_071742.1	R.MELLMFRFVHCHLLACEPK.T
5	6	2389.32388	0.5785	2.4640	2538	13/42	gi169215993ref XP_001726837.1	R.MELFLVFLTEGVSQALPESAK.G

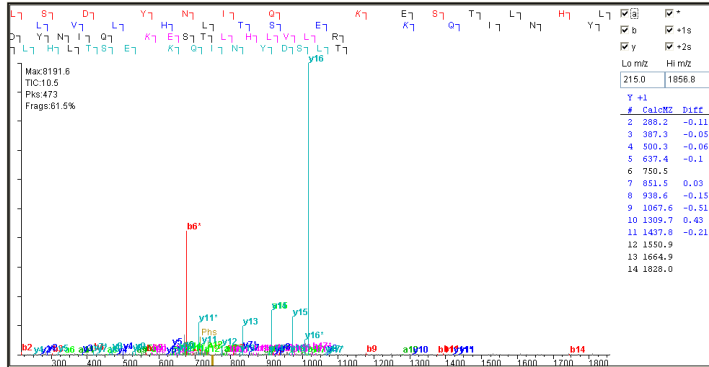


L Locus Description

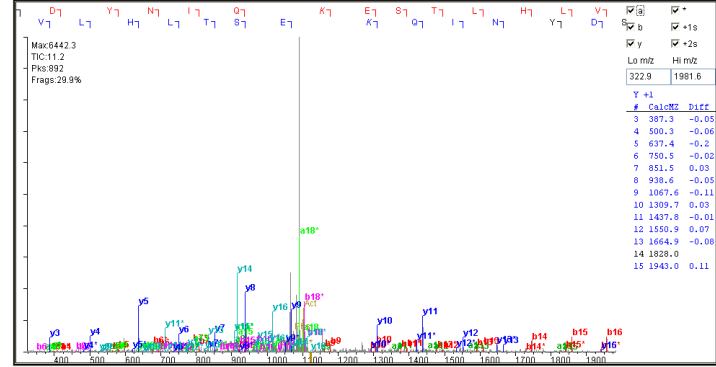
M	Residue Modified	Mass Difference	Sequence Alignment	XCorr	Filename	ModCount	Copy Count
L	psu PF13_0346	product=ubiquitin/ribosomal fusion protein uba52 homologue, putative					
L	psu PFL0585w						
M	63	114.04	TLSDYNIQESTLHLVLR	4.2151	Pf_Ring-ub-12h_25ug_OT-60K_Ti_108.011046.011046.3	1	21
M	63	114.04	TLSDYNIQESTLHLVLR	4.434	Pf_Schi-ub-36h_25ug_OT-60K_Ti_405.007752.007752.2	1	8

2244.20 amu Pf_Ring-ub-12h_25ug_OT-60K_Ti_108.011046.xxxxxx.3 db:/data1/proteomics/db/Pf_PlasmoDB_5.5_Hs_NCBI_2008-03-04_NR_wSHUFFLED_wNiP.fasta 2245.19 amu Pf_Schi-ub-36h_25ug_OT-60K_Ti_405.007752.xxxxxx.2 db:/data1/proteomics/db/Pf_PlasmoDB_5.5_Hs_NCBI_2008-03-04_NR_wSHUFFLED_wNiP.fasta

Rank	Sp	(M+H) ⁺	deltCn	XCorr	Sp	Ions	Reference	Peptide
1	1	2244.19879	0.0000	4.2151	10.474	26/68	psuPF13_0346	R.TLSDYNIQK*ESTLHLVLR.L
2	297	2244.15203	0.6390	1.5217	2.894	16/68	SHUFFLED_gi11038674refNP_000617.1	R.VQGSGLYIVIM#K*MYLVR.L
3	479	2243.14289	0.6488	1.4804	2.778	15/68	SHUFFLED_gi20127553refNP_057321.2	R.NSQM#LLIM#QVHLHLVLR.H
4	50	2242.22357	0.6632	1.4196	2.607	18/72	SHUFFLED_psuPF10455w	R.VLHDFNFKTKTNTFELTK.N
5	111	2240.09088	0.6750	1.3699	2.467	17/72	gi156616290refNP_001096078.1	R.VLHDFNFKTKTNTFELTK.K



Rank	Sp	(M+H) ⁺	deltCn	XCorr	Sp	Ions	Reference	Peptide
1	1	2244.19879	0.0000	4.4340	8.466	18/34	psuPF13_0346	R.TLSDYNIQK*ESTLHLVLR.L
2	2	2245.11539	0.4644	2.3747	3.754	14/32	gi38505215refNP_079316.2	R.THFPIVQNDTDLVYR*.N
3	9	2244.28681	0.5372	2.0519	3.015	12/36	gi169169346refNP_001718133.1	R.HFTVFR*LLTSLSPFLPFR.R
4	70	2245.17160	0.5506	1.9929	2.880	10/40	gi23957698refNP_705835.1	R.DTLGLFVAGLSEFVNGVLEK.T
5	13	2245.14329	0.5742	1.8881	2.640	12/38	gi34398348refNP_003880.3	R.TGTQLVGLVQGLTEEQRMIR.E



Unraveling the Ubiquitome of the Human Malaria Parasite

Nadia Ponts, Anita Saraf, Duk-Won D. Chung, Alona Harris, Jacques Prudhomme,
Michael P. Washburn, Laurence Florens and Karine G. Le Roch

J. Biol. Chem. 2011, 286:40320-40330.

doi: 10.1074/jbc.M111.238790 originally published online September 19, 2011

Access the most updated version of this article at doi: [10.1074/jbc.M111.238790](https://doi.org/10.1074/jbc.M111.238790)

Alerts:

- [When this article is cited](#)
- [When a correction for this article is posted](#)

[Click here](#) to choose from all of JBC's e-mail alerts

Supplemental material:

<http://www.jbc.org/content/suppl/2011/09/19/M111.238790.DC1.html>

This article cites 59 references, 16 of which can be accessed free at
<http://www.jbc.org/content/286/46/40320.full.html#ref-list-1>